Available online at www.sciencedirect.com
SCIENCE DIRECT®
NUCLEAR SCIENCE AND TECHNIQUES
Nuclear Science and Techniques, Vol.17, No.6 (2006) 334–341

Interaction between photons and electrons

JI Kai

(Institute of Materials Structure Science, High Energy Accelerator Research Organization (KEK), Graduate University for Advanced Studies, Oho 1-1, Tsukuba, Ibaraki 305-0801, Japan)

Abstract By using a path-integral theory, the photoemission spectra of the electron-phonon (e-ph) coupled systems are calculated exactly. The spectral properties of the e-ph coupled systems based on the 1D and 2D Holstein models are systematically studied under various conditions. The electronic band structure is found to be greatly modified by the multiple scattering effect of electron with phonons, so as to produce a spectral evolution from broad Gaussian at band bottom to two-headed Lorentzian near the Fermi energy. This evolution reflects a transition of electronic states from localized incoherent one to the extended coherent one near the Fermi energy. The results qualitatively agree with recent experiments of high resolution ARPES on the Be (0001) surface and $Bi_2Sr_2CaCu_2O_8$.

Key words Angle-resolved photoemission spectroscopy, Electron-phonon interaction, Synchrotron radiation

CLC number O485

1 Introduction

When a photon of synchrotron radiation is absorbed by a crystal, an electron in the crystal can possibly escape from the material and be detected by an electron energy analyzer. This process is the well-known photoelectron effect, which has become an advanced experimental technique nowadays in the study of the electronic properties of various materials.[1] In the momentum specified angle resolved photoemission spectroscopy (ARPES), the binding energy can now be measured as a function of each given momentum. With the rapid progress of this high resolution ARPES, now the electronic energy band structure can be discerned in the scale of a few meV. On the basis of this technical development, quite a few new properties associated with electron–phonon (e-ph) interaction have been discovered in the normal metallic states, as well as in the superconducting (SC) ones, signifying direct and clear evidences for the importance of the e-ph interactions.

It has been a long-standing question in solid state physics of how the e-ph interaction influences the electronic energy band structures, and finally determines a material to become an insulator, metal or superconductor. As ARPES can directly probe the structure of electronic energy bands and topology of Fermi surface, it has become one of the most important measurements for the experimental studies.

In the theoretical aspect, it is already known that these spectra are nothing but the Lehmann's representation of the one-body Green's function. In the case of a single electron coupled with phonons, it has been investigated in detail, by the ordinary perturbation theory, and also by the unitary transformation methods. As for the many-electron system coupled with phonons, the so-called Migdal–Eliashberg (ME) theory, and also adiabatic or mean field approximation are often used to clarify the energy band structures, in connection with various phase transition phenomena, such as the charge density wave (CDW) or SC state from the metallic one. In some cases, systematic theoretical methods have already been devised to take into account high order corrections, which are not included in the ordinary perturbation theories. However, these

Email: jikai@post.kek.jp.

existing theories seem to be not so useful to clarify the aforementioned ARPES, as it spans the whole momentum region from the Fermi one ($\equiv \boldsymbol{p}_F$) to the bottom of the valence band.

According to recent experimental results, it has become clear that the ARPES evolve quite drastically as the momentum changes from $\boldsymbol{p}_F$ to the band bottom. It is now well known, the ARPES on Be(0001) surface[2-4] and $Bi_2Sr_2CaCu_2O_8$ (Bi2212)[5] take sharp two-headed asymmetric Lorentzians at around $\boldsymbol{p}_F$, while becoming broad Gaussians at around the band bottom. These experiments clearly say that the electrons near $\boldsymbol{p}_F$ are in the coherent plane wave states, whereas at around the band bottom, they are in the incoherent quasi-localized states. This spectral evolution from the two-headed Lorentzian to the broad Gaussian, or from the coherent state to the incoherent one, is quite universal, and has become a basic problem of the e-ph coupling. However, its origin seems beyond the conventional approximation theories mentioned above. Thus, the problem how the e-ph interaction dominates the spectral shape has now emerged as a new challenge for the theory of solid state physics.

2 Model and methods

Recently, a new path-integral theory has been developed to calculate the ARPES of e-ph coupled systems[6,7]. The theory is free from any approximation, thus can well clarify the above-mentioned spectral features.

To investigate this problem, a many-electron system coupled with Einstein phonons, which is often called Holstein model[8], is taken:

$$H = -T\sum_{<i,j>}\sum_{\sigma}(a_{i\sigma}^{+}a_{j\sigma} + a_{j\sigma}^{+}a_{i\sigma}) - \mu\sum_{i,\sigma}a_{i\sigma}^{+}a_{i\sigma} + \sum_{i}\left(\frac{P_i^2}{2m} + \frac{1}{2}m\omega_0^2 Q_i^2\right) + S\sum_{i,\sigma}Q_i\left(n_{i\sigma} - \frac{\bar{n}}{2}\right) \quad (1)$$

Here $a_{i\sigma}^{+}$ and $a_{i\sigma}$ are the creation and annihilation operators for the conduction electron with a spin σ at site i. The total number of sites in a lattice is N, whereas the total electron number is N_e, and the average electron number per site is $\bar{n}$. T is the transfer energy, and μ the chemical potential of electrons. In this model, the electrons hop between two nearest neighboring sites (see Fig. 1), denoted by <i, j>, and couple to the Einstein phonons, which are localized at each site i.P_i and Q_i are the momentum and coordinate operators for this phonon at the site i, with a frequency ω_0 and a mass m. S is the coupling constant of this e-ph interaction.

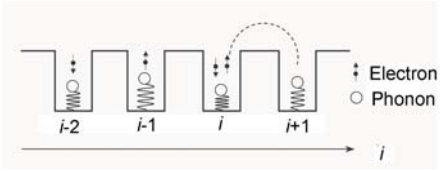

Fig. 1 Schematic diagram for the electron-phonon coupled system (Holstein model).

The Holstein model has been studied extensively, with various interests ranging from the competition between metallic, CDW, and SC phases, to the energy gap opening, by perturbative[9-13] and non-perturbative[14-17] methods. In the numerical study, the path-integral is performed by the quantum Monte Carlo (QMC) simulation. Hence, the results are exact. In the calculation, both metallic and CDW states have been considered. However, as the characteristic spectral evolution described above has been observed only in the gapless states, the present study will focus mainly on the metallic phases, and restrict attention to the weak and intermediately coupled e-ph systems with a little high temperatures, i.e., $\theta = 20 \sim 25$ ($\theta \equiv 1/k_B T$). In this regard, the CDW or SC gap opening will not be fully addressed.

From the theoretical point of view, the spectral function can be obtained from the single-particle Green's function:

$$G_{i,j,\sigma}(\tau) = -\left\langle T_\tau a_{i\sigma}(\tau)a_{j\sigma}^{+}\right\rangle \quad (2)$$

where τ means imaginary time, $a_{i\sigma}(\tau)$ is the Heisenberg representation of $a_{i\sigma}$, and T_τ is the time ordering operator. In this theory, the Green's function of Eq. (2) is calculated by the hybrid quantum Monte Carlo (QMC) simulation method[18] with a leap-frog algorithm[19]. After the Fourier transformation of Green's function

$$G_\sigma(\boldsymbol{p},\tau) = \frac{1}{N}\sum_{i,j}\mathrm{e}^{\mathrm{i}\boldsymbol{p}\cdot(\mathrm{R}_i - \mathrm{R}_j)}G_{i,j,\sigma}(\tau) \quad (3)$$

the electronic spectral function [$\equiv A_\sigma(\boldsymbol{p},\omega)$] can be obtained through the analytic continuation[20,21] as

$$G_\sigma(\boldsymbol{p},\tau) = \int_{-\infty}^{\infty}\frac{\mathrm{e}^{-\omega\tau}}{1+\mathrm{e}^{-\omega\theta}}A_\sigma(\boldsymbol{p},\omega)\,\mathrm{d}\omega \quad (4)$$

3 Conventional theories for e-ph interaction

Generally speaking, when an electron is added to (or removed from) the interacting N-electron system, an excited state with the electron (or hole) is created in the solid. This excited state is not stable and soon decays into lower energy states because of the interaction with the nearby particles. As a result, the high-energy electron (hole) evolves to a lower energy one, together with virtual excitations around it. This dressed particle can be viewed as a quasiparticle. In the e-ph coupled case, it is called a polaron.

Before a detailed analysis of the QMC results on the ARPES, a brief review is first given on the conventional mean-filed and perturbative methods for the e-ph coupled system and its spectral function. In Hamiltonian (1), if the e-ph coupled term is rewritten into the following form:

$$Q_i n_{i\sigma} \rightarrow Q_0 n_{i\sigma} + Q_i \frac{\overline{n}}{2} - Q_0 \frac{\overline{n}}{2}$$

where Q_0 is the average of phonon displacement Q_i on each lattice site, then a formally decoupled Hamiltonian is obtained for the electronic part and the eigen energy $E(\boldsymbol{p})$easily calculated. In this way, the electronic spectral function becomes

$$A_\sigma(\boldsymbol{p},\omega) = \delta[\omega - E(\boldsymbol{p})] \tag{5}$$

which takes a form of δ function, located at the electronic bonding energy of $E(\boldsymbol{p})$, as shown in Fig. 2(a).

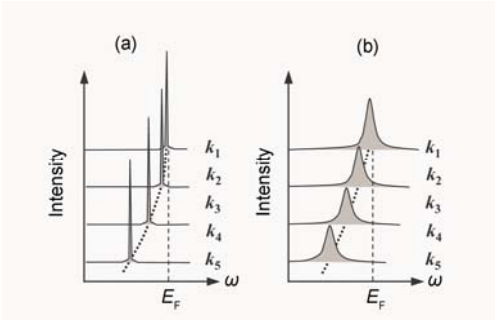

Fig.2 ARPES calculated by the conventional theories. (a) Mean-field approximation. (b) Perturbative method.

The above treatment is called the mean-field approximation. Obviously, it is easy to carry out. However, as it treats the lattice distortion uniformly, only the global lattice shift is considered here [see in Fig. 3(a)]. In this sense, the local lattice distortion and polaron effect cannot be described by this method.

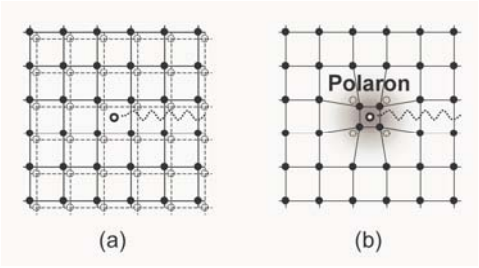

Fig.3 The e-ph coupling effects described by different theories. (a) In the mean-field approximation, the lattice is shifted uniformly as an electron propagates in the crystal. (b) In the perturbative method, the electron causes only a local lattice distortion around it, leading to the formation of polaron.

Another approach to the e-ph model is the perturbative method.[22,23] Within the perturbative theory, the spectral function $A_\sigma(\boldsymbol{p},\omega)$ for the added (removed) electron is related to the electronic self-energy $\Sigma_\sigma(\boldsymbol{p},\omega)$ ($\equiv \Sigma_\sigma^R(\boldsymbol{p},\omega) + \mathrm{i}\Sigma_\sigma^I(\boldsymbol{p},\omega)$) by

$$A_\sigma(\boldsymbol{p},\omega) = -\frac{\Sigma_\sigma^I(\boldsymbol{p},\omega)}{\pi\left\{\left[\omega - \varepsilon_{\mathbf{k}} - \Sigma_\sigma^R(\boldsymbol{p},\omega)\right]^2 + \left[\Sigma_\sigma^I(\boldsymbol{p},\omega)\right]^2\right\}} \tag{6}$$

The self-energy $\Sigma_\sigma(\boldsymbol{p},\omega)$ represents the energy change of electron when it induces a local lattice distortion around it because of the e-ph interaction, as shown in Fig. 3(b). Thus it plays an important role in describing the polaron effect on the ARPES of the N-electron system. In the noninteracting limit $S \rightarrow 0$, $\Sigma_\sigma(\boldsymbol{p},\omega) = 0$, and the spectral function (6) is reduced to a δ function:

$$A_\sigma(\boldsymbol{p},\omega) = \delta(\omega - \varepsilon_p) \tag{7}$$

corresponding to a real particle with an energy $\omega = \varepsilon_{\mathbf{p}}$, where $\varepsilon_{\mathbf{p}}$ is the energy for the noninteracting electron of momentum $\boldsymbol{p}$. When the e-ph interaction is switched on, the spectral function of Eq. (6) is characterized by a Lorentzian lineshape, which is peaked at $\omega = \varepsilon_{\mathbf{p}} + \Sigma_\sigma^R(\boldsymbol{p},\omega)$ with half-width $\Sigma_\sigma^I(\boldsymbol{p},\omega)$ (see in Fig. 2(b)). This structure corresponds to a polaron consisting of an electron with a phonon cloud around itself. The mass of this composite particle is renormalized by the self-energy. Besides, according to the uncertainty principle, the lifetime of the quasiparticle is inversely proportional to the peak width.

For the case of e-ph system, the Feynman diagram expansion (perturbation) theory is often applied to obtain the self-energy $\Sigma_\sigma(\boldsymbol{p},\omega)$ within the ME approximation. By this means, the e-ph system in the normal and superconducting states has been studied.

However, if the coupling is not weak, the high order terms may have equal importance as the lower ones. Thus, in the strong coupling region, complex phonon exchange between electrons cannot be omitted, and the ME approximation breaks down.

4 Theoretical results of ARPES

As ARPES probes the occupied electronic state in the crystal, its intensity ($\equiv I(\boldsymbol{k},\omega)$) is related to the spectral function $A_\sigma(\boldsymbol{p},\omega)$ by

$$I(\boldsymbol{p},\omega) = \sum_\sigma A_\sigma(\boldsymbol{p},\omega) f(\omega) \tag{8}$$

where the Fermi function $f(\omega) = 1 / (\exp(\theta\omega) + 1)$ is imposed.

As mentioned before, one of the most interesting properties revealed by the high resolution ARPES on the e-ph coupled system, is the case of beryllium (0001) surface state, in which a strong side peak seemingly because of this e-ph coupling has been observed. The surface state of Be(0001) is significantly different from the bulk Be. The band structure calculation shows that the Fermi level ($\equiv E_F$) of bulk Be is situated in a dip of the density of states of electrons.[24] The low density of free charge carrier makes Be an exceptional semi metal rather than the normal conductors.[25] Whereas only at the surface layer, the electron becomes more free-electron-like because of a high electronic density of this surface states.[26] This feature makes Be surface a fairly good metallic plane unlike the almost insulating bulk state.[27, 28]

In addition to the substantial earlier research work with ARPES, low-energy electron diffraction and electron-energy-loss spectroscopy, contemporary studies of Be surface electronic structure have advanced into the level of a few meV near E_F with the aid of high-resolution ARPES. In Ref.[2], Hengsberger *et al*. reported the ARPES measurements of the Be(0001) surface state. In that experiment, it was observed that the spectra of high binding energy have the broad Gaussian distribution. It means that the electron in this state is almost localized as being incoherent. Whereas, as the binding energy approaches towards E_F, a small shoulder appears. Close to E_F, the shoulder gains more spectral weight and the whole spectral shape exhibits an asymmetric Lorentzian of a two-headed structure. It means the electron in this state is almost coherent with a plane wave nature extending over all the crystal. The broad Gaussian around band bottom and the side peak near E_F are attributed to the strong e-ph interaction instead of the CDW or surface superconductivity, as no energy gap was observed down to 12K. Later, this result was confirmed by LaShell *et al*.[4] who independently performed the same experiment.

Moreover, similar systematic change from Gaussian to two-headed asymmetric Lorentzian shape was also observed in several other materials. For example, in the case of $Bi_2Sr_2CaCu_2O_8$ (Bi2212),[5] the double-peaked structure is clearly displayed and leads to a 'dip-hump' structure near E_F. As other mechanisms were ruled out, it was concluded that the reason for this spectral change could only be the strong e-ph interaction.

From these experimental results, it is found that the characteristic spectral evolution from broad Gaussian to two-headed asymmetric Lorentzian appears quite universal for a wide variety of e-ph systems in the metallic states. However, its origin seems difficult to clarify by the conventional perturbation theories, such as the ME approximation. This difficulty comes from a common failing of the perturbative methods, that is, the high-order contributions of complicated phonon exchange processes between electrons are not properly considered in these theories. Whereas, in the path-integral theory, all kinds of e-ph scattering processes can be taken into account, and so, the calculation is expected to well clarify the origin of the aforementioned spectral evolution.

In Fig. 4, the results of $I(\boldsymbol{p},\omega)$ of 1D Holstein model at 29.17%-filling (48 sites with 28 electrons) for two different e-ph coupling constants are shown. The panel (a) corresponds to $S = 0.8$, and (b) $S = 1.0$. The inverse temperature is $\theta = 20$. The phonon effective mass is taken as $m = 80$ here. From panel (a) it is seen that the spectrum takes a broad Gaussian near the band bottom $\boldsymbol{p} = 0$. As $\boldsymbol{p}$ increases, the peak width gradually decreases, and at $\boldsymbol{p}_F = 7\pi/24$, the spectrum shows a slightly two-headed Lorentzian. In the panel (b), S is increased, thus the spectra close to the band bottom are further broadened. Whereas near $\boldsymbol{p}_F$, a second peak (referred to as phonon peak in the following)

appears, and the whole spectrum has become a two-headed asymmetric Lorentzian. These behaviors are well consistent with the aforementioned experimental discoveries, although the agreement between the theory and the experiments are qualitative.

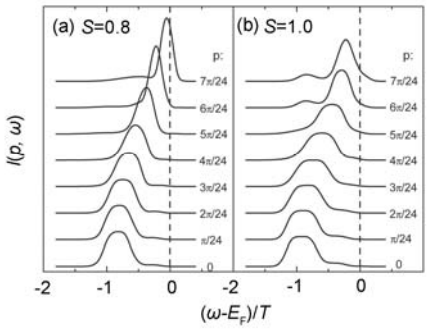

Fig.4 QMC results of ARPES of 1D Holstein model at 29.17%-filling (48 sites with 28 electrons) for different e-ph coupling constants *S*. Parameters are: $\theta = 20$, $T = 1.0$, $\omega_0 = 0.1$, $m = 80$.

In Fig. 5, the QMC results for the 2D case along the ΓM symmetry line of the Brillouin zone at 35.94%-filling (8×8 square lattice with 46 electrons) for two different coupling constants are shown. The panel (a) is for $S = 0.8$, and (b) is $S = 1.0$. θ is the same as that of Fig. 4. Although the simulation on the 8×8 system gives only a limited number of $\boldsymbol{p}$'s, the main feature of the aforementioned spectral evolution is well displayed here. Near the band bottom, the spectra have a broad Gaussian shape, whereas at $\boldsymbol{p}_F$, the spectra show an asymmetric Lorentzian form. With the increase of coupling constant, the spectra at $\boldsymbol{p}_F$ change from a slightly two-headed form to a clear two-headed one. These results are qualitatively in good agreement with the experimental observations.

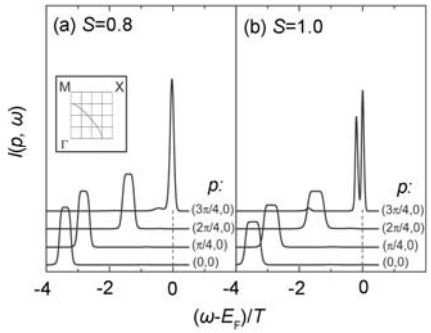

Fig.5 QMC results of ARPES of 2D Holstein model at 35.94%-filling (8×8 square lattice with 46 electrons) along the ΓM direction for different e-ph coupling constants *S*. Parameters are: $\theta = 20$, $T = 1.0$, $\omega_0 = 0.1$, $m = 80$. The inset in (a) shows the Brillouin zone and the Fermi surface. The grid box represents the resolution for the QMC simulation.

In Fig. 6, the temperature dependence of spectra is presented for the 2D case at 35.94%-filling (8×8 square lattice with 46 electrons). The panel (a) is for $\theta = 20$, and (b) for $\theta = 25$. The e-ph coupling constant is fixed at $S = 0.8$. In comparison with Fig. 5, it is seen that decreasing temperature also brings about a notable phonon peak at $\boldsymbol{p}_F$. Whereas, as the thermal broadening is suppressed at low temperature, in the panel (b), the spectral shape becomes narrower and sharper. It can also be said that some fine structure, obscured in the panel (a), becomes more pronounced under the low temperature condition (b). For example, a small hump appears in the spectrum $\boldsymbol{p} = (2\pi/4, 0)$. In the inset, this small peak with clear error bars has been zoomed into. Here it is clearly seen that these weak structures are not numerical errors, but are other phonon peaks.

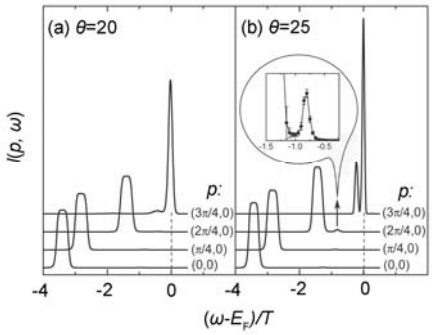

Fig.6 QMC results of ARPES of 2D Holstein model at 35.94%-filling (8×8 square lattice with 46 electrons) along the ΓM direction for different temperatures θ. The inset magnifies the small hump denoted in (b). Parameters are: $S = 0.8$, $T = 1.0$, $\omega_0 = 0.1$, $m = 80$.

From Figs. 4–6, it is seen that the results are quite consistent with the experimental spectra. The next section will try to show the microscopic origin for these phonon peaks and spectral evolution.

5 General description of band structure

If the spectral functions $A_\sigma(\boldsymbol{p},\omega)$ are placed side by side as a function of momentum $\boldsymbol{p}$, then a graph of intensity map such as Fig. 7 results, from which the band structure is known with ease. In Fig. 7(a), the intensity map of 1D Holstein model at 29.17%-filling (48 sites with 28 electrons), with $S = 0.8$, $T = 1.0$, $\omega_0 = 0.1$, $\theta = 20$, $m = 80$ is presented. In Fig. 7(b), the skeleton image of the energy bands obtained by connecting the peak maxima in (a) is shown. In the panel (a),

the cosine-shaped main bands are easily recognized. In the panels (b), the corresponding one is denoted by the solid line, and the half-width of the cosine band is schematically shown by the error bars. In addition to the main band, the phonon bands can also be seen in the intensity map (a). They are outlined by the dash lines in the skeleton image (b).

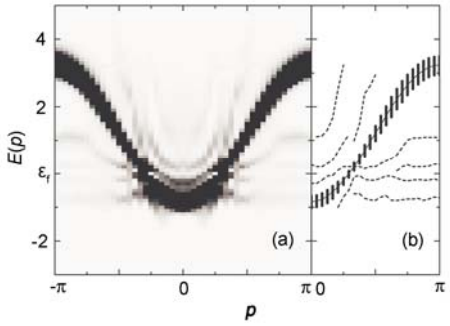

Fig.7 Band structure of 1D Holstein model at 29.17%-filling (48 sites with 28 electrons), with $S = 0.8$, $T = 1.0$, $\omega_0 = 0.1$, $\theta = 20$, $m = 80$. Panel (a) is the intensity map of QMC raw data. (b) is the skeleton image of the energy bands obtained by connecting the peak maxima shown in (a). The solid line corresponds to the main band, and the error bars denote its half-width. The phonon bands are shown by the dash lines.

In these figures, $\boldsymbol{p}$ is nothing but the momentum of the added hole or electron in the N-electron system, and $E(\boldsymbol{p})$ is the polaron energy. These graphs of band structure can be understood from the view of the recoil effect of the electron[29] (here the interpretation is confined within the case of the hole left under E_F after the photo excitation. Note that the hole-phonon interaction is the same as the electron-phonon interaction). In the e-ph system, the motions of electron and phonon are mutually interfered. The motion of phonons changes the potential field felt by the electron, whereas the electron also changes the potential exerted on the phonon. As a result, the instaneous status of the electron and phonon is always changing. What is exactly known is only the total polaron momentum $\boldsymbol{p}$, which is conserved during the e-ph scattering. Hence the spectrum for each momentum $\boldsymbol{p}$ provides a picture of the entangled electron and phonon, i.e., the polaron.

In the noninteracting limit, no phonon is emitted or absorbed, and the total polaron energy of momentum $\boldsymbol{p}$ is equivalent to the electron energy, $E(\boldsymbol{p}) = \varepsilon_{\mathbf{p}}$. When the e-ph interaction is introduced, the total polaron energy is also changed from $\varepsilon_{\mathbf{p}}$. For example, it becomes $\varepsilon_{\mathbf{p+q}} + \omega_{\mathbf{-q}}$ after the hole emits a phonon of momentum $-\boldsymbol{q}$ and is recoiled from $\varepsilon_{\mathbf{p}}$ to $\varepsilon_{\mathbf{p+q}}$. This state may correspond to a new peak at $E(\boldsymbol{p}) = \varepsilon_{\mathbf{p+q}} + \omega_{\mathbf{-q}}$ away from the main peak at $E(\boldsymbol{p}) = \varepsilon_{\mathbf{p}}$ (see in Figs. 8(a) and 8(b)). One can expect that small energy change because of phonon creation or annihilation only contributes to the broadening of the main band, and dramatic change gives rise to some new phonon bands. If more phonons are involved in this process, the main band (as well as phonon bands) can be further broadened, and more phonon bands can be formed.

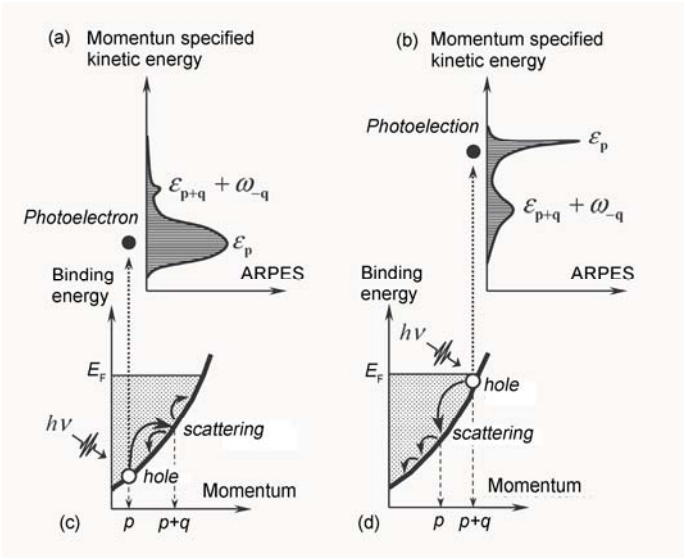

Fig.8 ARPES and the dynamics of multiple scattering in the e-ph coupled system. In the panel (c), a hole is created near the band bottom after the photo excitation, and (d) is the case close to the Fermi surface. The lower panels (c) and (d) show the scattering processes in the electronic band. The upper panels (a) and (b) are the corresponding spectral densities. See the text for details.

The energy difference of electron because of e-ph scattering can be estimated by $\Delta E = \nabla_{\mathbf{q}} E(\boldsymbol{p}) \cdot \Delta \boldsymbol{p}$, where $\Delta \boldsymbol{p}$ comes from the momentum exchange with phonon. For the case of cosine band, $E(\boldsymbol{p}) \sim -\sum_i \cos(\boldsymbol{p}_i)$, so ΔE is small near the band bottom, and the e-ph scattering mainly contributes to the broadening effect. Some weak phonon peaks can only be seen to the lower energy side of the cosine band (Fig. 8(a)), this is because $\varepsilon_{\mathbf{p+q}} + \omega_{-\mathbf{q}}$ is always less than $\varepsilon_{\mathbf{p}}$ (allowing for that in the normal state, phonon energy $\omega_{\mathbf{q}}$ is negligible for the electron). For the scattering near E_F, ΔE can be relatively large, which favors creating new phonon peaks. These peaks, in this case, appear only to the high binding energy side [Fig. 8(b)], as the hole cannot be scattered into the empty band above E_F. The scattering can also occur between E_F and band bottom, and hence the phonon bands above and below the cosine band can both be produced.

A hole just under E_F is the most stable one in the energy band. At that position, the hole can easily settle down without much virtual phonon excitation. So if an electron is excited from somewhere near E_F, its spectral shape of photoemission will be almost free-electron-like and take a sharp Lorentzian form (Fig. 8(b)). Whereas, if an electron is excited from the band bottom, the high energy hole left at the band bottom will induce thick phonon cloud around it. As a result, the spectral shape is heavily modified by the e-ph interaction and has a broad Gaussian distribution (Fig. 8(a)). A statistical average over all the procedures described above then gives the spectral evolution of ARPES.

6 Summary

In this lecture, a new path-integral theory is developed to calculate the photoemission spectra of the e-ph coupled systems. The imaginary time Green's function of electron is calculated, from which the spectral function is reproduced by the analytic continuation. By this means, the spectral properties of the e-ph coupled systems based on the 1D and 2D Holstein models are systematically studied under various conditions. The band structure is found to be greatly modified by the multiple scattering effect of electron with phonons, even if the whole system is still metallic and the e-ph coupling strength is intermediate. Around the band bottom, the spectrum takes a broad Gaussian, indicating the electron in this state is nearly localized and incoherent. Whereas near the $\boldsymbol{p}_F$, the spectral shape is characterized by an asymmetric two-headed Lorentzian, which means the electron in this state is almost coherent with a plane wave nature, extending over all the crystal. The results qualitatively agree with recent experiments of high resolution ARPES on the Be (0001) surface and $Bi_2Sr_2CaCu_2O_8$.

References

1 Hüfner P, Photoelectron spectroscopy, 3rd ed. Berlin:Springer, 2003.

2 Hengsberger M, Purdie D, Segovia P, *et al*. Phys. Rev. Lett. 1999, **83**:592.

3 Hengsberger M, Frésard R, Purdie D, *et al*. Phys. Rev. 1999, **B60**:10796.

4 LaShell S, Jensen E, Balasubramanian T, Phys. Rev. 2000, **B61**:2371.

5 Lanzara A *et al*., Nature. 2001, **412**:510.

6 Nasu K, J. Phys. Soc. Jpn. 1996, **65**:2285.

7 Ji K, Zheng H, Nasu K, Phys.Rev. 2004, **B70**:085110.

8 Holstein T, Ann. Phys. (N.Y.), 1959, **8**:325.

9 Miller P, Freericks J K, Nicol E J, Phys. Rev. 1998, **B58**:14498.

10 Lang I G, Firsov Y A, Sov. Phys. JETP. 1963, **16**:1301.

11 Meyer D, Hewson A C, Bulla R, Phys. Rev. Lett. 2002, **89**:196401.

12 Ku L-C, Trugman S A, Bonca J, Phys. Rev. 2002, **B65**:174306.

13 Monthoux P, Scalapino D J, Phys. Rev. 2002, **B65**:235104.

14 Weiße A, Fehske H, Phys. Rev. 1998, **B58**:13526.

15 Jeckelmann E, White S R, Phys. Rev. 1998, **B57**:6376.

16 Hirsch J E, Fradkin E, Phys. Rev. 1983, **B27**:4302.

17 Noack R M, Scalapino D J, Scalettar R T, Phys. Rev. Lett. 1991, **66**:778.

18 Duane S, Kennedy A D, Pendleton B J, *et al*. Phys. Lett. 1987, **B195**:216.

19 Allen M P, Tildesley D J, Computer simulation of liquids. Oxford: Clarendon, 1987.

20 White S R, Scalapino D J, Sugar R L, *et al*. Phys. Rev. Lett. 1989, **63**:1523.

21 Gubernatis J E, Jarrell M, Phys. Rep. 1996, **269**:135.

22 Migdal A B, Sov. Phys. JETP. 1958, **7**:996.

23 Eliashberg G M, Sov. Phys. JETP, 1960, **11**:696.

24 Chou M Y, Lam P K, Cohen M L, Phys. Rev. 1983, **B28**:4179.
25 Inoue S T, Yamashita J, J. Phys. Soc. Jpn. 1973, **35**:677.
26 Feibelman P J, Stumpf R, Phys. Rev. 1994, **B50**:17480.
27 Chulkov E V, Silkin V M, Shirykalov E N, Surf. Sci. 1987, **188**:287.
28 Hannon J B, Mele E J, Plummer E W, Phys. Rev. 1996, **B53**:2090.
29 Mahan G D, Many-particle physics, 2nd ed. New York: Plenum, 1990.